

# Model for crankshaft motion of protein backbone in nonspecific binding site of serine proteases

A.E. Sitnitsky,

*Kazan Institute of Biochemistry and Biophysics, P.O.B. 30, Kazan 420111,  
Russia. e-mail: sitnitsky@mail.knc.ru*

---

## Abstract

The consequences of recent experimental finding that hydrogen bonds of the anti-parallel  $\beta$ -sheet in nonspecific binding site of serine proteases become significantly shorter and stronger synchronously with the catalytic act are examined. We investigate the effect of the transformation of an ordinary hydrogen bond into a low-barrier one on the crankshaft motion a peptide group in the anti-parallel  $\beta$ -sheet. For this purpose we make use of a realistic model of the peptide chain with stringent microscopically derived coupling interaction potential and effective on-site potential. The coupling interaction characterizing the peptide chain rigidity is found to be surprisingly weak and repulsive in character. The effective on-site potential is found to be a hard one, i.e., goes more steep than a harmonic one. At transformation of the ordinary hydrogen bond into the low-barrier one the frequency of crankshaft motion of the corresponding peptide group in the anti-parallel  $\beta$ -sheet is roughly doubled.

*Key words:* peptide group, protein, backbone, serine protease.

---

## 1 Introduction

The problem of localization and storage of energy by proteins at binding of ligands or protein-protein interactions is an old one in biophysics (for review see [1], [2] and refs. therein). This problem is especially urgent within the context of enzymatic catalysis. How does an enzyme store and utilize the energy released at substrate binding? The answer to this question is very poorly understood not only at quantitative but even at qualitative level. In

---

*Email address:* sitnitsky@mail.knc.ru (A.E. Sitnitsky).

our opinion recent experimental data on serine proteases [3] are able to shed light on this problem.

Indeed the high resolution X-ray diffraction studies ( $\leq 1.2 \text{ \AA}$ ) of serine protease intermediate structures revealed that "the strength of the hydrogen bonds between the enzyme and the substrate changed during catalysis. The well-conserved hydrogen bonds of antiparallel  $\beta$ -sheet between the enzyme and the substrate become significantly shorter in the transition from a Michaelis complex analogue ... to an acyl-enzyme intermediate ... presumably synchronously with the nucleophilic attack on the carbonyl carbon atom of the scissile peptide bond. This is interpreted as an active mechanism that utilizes the energy released from the stronger hydrogen bonds to overcome the energetic barrier of the nucleophilic attack by the hydroxyl group of the catalytic serine." [3]. It is worthy to note that these data are in coherence with those of [4] (see also [5] and refs. therein) that the  $\beta$ -strand corresponding to residues 214–217 shifts  $\sim 0.8 \text{ \AA}$  toward the inhibitor upon its binding by  $\alpha$ -lytic proteases. Here one should strictly discriminate the established experimental fact of the hydrogen bonds shortening and strengthening in the antiparallel  $\beta$ -sheet from the speculation about the participation of this effect in the mechanism of the catalysis. The latter is an intriguing hypothesis that still needs to be confirmed. It will not be touched upon in the present paper. Our concern here is in modeling the consequences of the hydrogen bonds shortening and strengthening in the antiparallel  $\beta$ -sheet for its dynamics.

Serine proteases are the most extensively investigated enzymes (for review see [6], [7] and refs. therein). The greatest wealth of structural and kinetic data has been obtained for them. That is why these "working horses" of enzymology are the most suitable objects for investigating unresolved problems of enzymatic catalysis. The antiparallel  $\beta$ -sheet mentioned above forms the non-specific binding site of serine proteases and is quite similar for all of them. The differences are in specific binding sites which are of no interest for us here. The antiparallel  $\beta$ -sheet of the nonspecific binding site comprises three sequential peptide groups of enzyme backbone which form hydrogen bonds with corresponding peptide groups of the substrate (see Fig.3 in [6] or a schematic picture Fig.24-9 in [8] or that Fig.11.6 in [9]). Despite the fact that two peptide chains belong to two different proteins the resulting structure has all features of the antiparallel  $\beta$ -sheet and is usually called so without reserve.

Nature of hydrogen bonds in proteins is a matter of controversy from the beginning of protein science and enzymology. In particular the possibility of the so-called low barrier hydrogen bonds in enzyme active sites is of utmost interest. The proposal about their role for enzymes was put forth by Gerlt, Clealand and Frey in 1993-1994 (for review see [10], [11] and refs. therein). Since then their participation in transition state stabilization is a matter of heated debates [12], [13]. Especially that between His and Asp in the catalytic

triad of serine proteases remains to be the subject of numerous studies and non-stopping controversy with arguments pro [14],[15], [16], [17], [18], [19], [20], [21], [22] and contra [5], [13], [23]. We do not touch upon the catalytic triad in the present paper and focus ourselves exclusively on the processes in the nonspecific binding site. The most salient feature of low barrier hydrogen bonds as compared to ordinary hydrogen bonds is their strength and short distance between hydrogen donor and acceptor atoms (dDA). We do not involve ourselves in very intricate classification debates about blurred boundaries between weak, strong, short strong, short ionic, low barrier and very strong hydrogen bonds (see, e.g., [24]). For convenience we freely divide the hydrogen bonds to strong ones (SHB) and weak ones (WHB). We set that SHB have energies  $\geq 10$  kcal/mol and dDA  $\leq 2.5$  Å while WHB have energies  $2 \div 5$  kcal/mol and dDA  $\geq 2.8$  Å. Thus the aim of the present paper is to investigate the transformation of WHB into SHB in the antiparallel  $\beta$ -sheet of the nonspecific binding site of serine proteases. To be more precise we study the effect of this transformation on the backbone dynamics in the antiparallel  $\beta$ -sheet. However it should be stressed that following [24] we believe that there are no well defined boundaries between different types of hydrogen bonds. In fact we investigate the parametric dependence of the backbone dynamics on the hydrogen bond energy from the range  $2 \div 30$  kcal/mol.

Last years are marked by noticeable progress in revealing subtleties of protein dynamics gained by infra-red (IR) spectroscopy [25], [26], [27], [28], [29], [30], normal mode analysis [31], [32], [33] and molecular-dynamics simulations (see the recent reviews [34], [35] and refs. therein). There are several analytical models treating mechanics of peptide chain backbone [36], [37], [38], [39]. The most interesting type of motion for our context is the so the so called "crankshaft-like" one. It means the rocking of the rigid plane of the peptide group due to degrees of freedom of torsional (dihedral) angles  $\varphi_i$  and  $\psi_{i-1}$  (see Fig.1). It was proposed on theoretical grounds from normal-mode analysis [40] and is supported by NMR experiments and molecular dynamics simulations of protein backbone [41], [42], [43], [44], [45], [46], [47], [48], [49], [50], [51], [52], [53], [54]. It is comprehended now as a dominant type of motion for the latter that "involves only a localized oscillation of the plane of the peptide group. This motion results in a strong anticorrelated motion of the  $\Phi$  angle of the  $i$ -th residue ( $\Phi_i$ ) and the  $\Psi$  angle of the residue  $i - 1$  ( $\Psi_{i-1}$ ) on the 0.1 ps time scale." [54]. Thus the essence of this motion is the so called anticorrelated motion of the torsional angles  $\varphi_i$  and  $\psi_{i-1}$  manifested itself in the requirement (see Fig.2)

$$\phi/2 \equiv \Delta\varphi_i = \Delta\psi_{i-1}$$

In this case the plane of the peptide group rocks as a whole around some axis  $\sigma$  that goes through the center of masses of the peptide group parallel to the

bonds  $C_{\alpha}^{i-1} - C^i$  and  $N^i - C_{\alpha}^i$  (see Fig.1). The moment of inertia of the peptide group relative to the axis  $\sigma$  can be easily calculated to be  $I \approx 7.34 \cdot 10^{-39} g \cdot cm^2$  (see Appendix). Molecular dynamics simulations and NMR experimental data suggest that the character of the correlation function for the crankshaft motion is decaying oscillations [43], [54] but provide characteristics for them in a very wide range from the subpicosecond and picosecond time scale [54] to slower motions on a much larger time scale from tens of picoseconds to 100 ps and more [53]. This is presumably a manifestation of the "Russian doll" structure of the conformational potential for the crankshaft motion when a group of local minima forms a smooth local minimum and so on. In fact knowing the actual values of the frequency for the oscillations and the characteristic time of their decay for the functionally important crankshaft motion is not indispensable for the purposes of the present paper. However in our opinion it is reasonable to assume that the frequency of oscillations of the plane of the peptide group as a whole for such motion should be at least order of magnitude less than those for high frequency in - plane motions such as, e.g., Amide-I ( $\sim 1600 \text{ cm}^{-1}$ ). The choice of the frequency in the  $\omega_0 \sim 100 \text{ cm}^{-1} \approx 10^{13} \text{ s}^{-1}$  range enables us to match it with the amplitudes of rocking of order of several degrees (see (12) below) in accordance with experimental data [50], [52].

To investigate the effect of the transformation of WHB into SHB in the antiparallel  $\beta$ -sheet on the characteristics of the backbone crankshaft motion we use the model developed earlier [55], [56]. The latter is a microscopically stringent model of polypeptide backbone dynamics. It deals with realistic effective on-site potentials and coupling interaction potentials but at the same time is simple and tractable. The model yields for the correlation function of the crankshaft motion the exponentially decaying oscillations [56] in qualitative agreement with the results of molecular dynamics simulations [54]. The model enables us to elucidate the role of hydrogen bonds in the backbone dynamics.

The paper is organized as follows. In Sec.2 the Hamiltonian of the model is constructed. In Sec.3 the coupling interaction of two adjacent peptide groups is considered. In Sec.4 the local on-site potential for the peptide group is considered. In Sec.5 the contribution of hydrogen bonds is separately considered because they are the central point of the present paper. In Sec.6 the dimensionless characteristics of the effective on-site potential and of the coupling interaction potential are discussed. In Sec.7 the equation of motion is derived and the correlation function for crankshaft motion is obtained. In Sec.8 the results are discussed and the conclusions are summarized. In Appendix some technical details are presented.

## 2 The Hamiltonian of the model

A schematic picture of a polypeptide chain with all designations used further is presented in Fig.1. The mutual orientation of two adjacent peptide groups is characterized by the torsional (dihedral) angles  $\varphi_i$  and  $\psi_i$ . The angle  $\varphi_i$  characterizes the rotation round the bond  $C_i^\alpha - N_i$  and that  $\psi_i$  characterizes the rotation round the bond  $C_i^\alpha - C_i'$ . Further we consider the equilibrium dynamics in the antiparallel  $\beta$ -sheet for which the equilibrium values of the torsional angles are the same for all peptide groups (they are listed at the end of the next Sec.). We consider small deviations  $\varphi_i(t)$  and  $\psi_i(t)$  of the torsional angles from their equilibrium values ( $\varphi_i = \varphi_i^0 + \varphi_i(t)$  and  $\psi_i = \psi_i^0 + \psi_i(t)$ ) with  $|\varphi_i(t)| \leq 20^\circ$  and  $|\psi_i(t)| \leq 20^\circ$ . At such amplitudes of the deviations the hydrogen bonds confining the peptide group in the antiparallel  $\beta$ -sheet are not broken [8]. Finally we consider a peculiar type of motion  $\psi_{i-1}(t) = \varphi_i(t)$  that is namely the crankshaft one. The latter means that the peptide group rotates as a whole respective some effective axis  $\sigma$  passing through the center of the C–N bond parallel to the bonds  $C_i^\alpha - C_i'$  and  $N_{i+1} - C_{i+1}^\alpha$  that are assumed to be approximately parallel ( $\angle C_i^\alpha - C_i' - N_{i+1} = 113^\circ$  and  $\angle C_i' - N_{i+1} - C_{i+1}^\alpha = 123^\circ$  [57]). This type of motion is stipulated by the fact that the peptide group is a planar rigid structure [8], [57]. For the sake of uniformity of designations we further denote  $x_i = 2\varphi_i(t) = 2\psi_{i-1}(t)$  (see Fig.2) and thus

$$\varphi_i = \varphi_i^0 + x_i/2; \quad \psi_{i-1} = \psi_{i-1}^0 + x_i/2 \quad (1)$$

The moment of inertia of the peptide group relative to the axis  $\sigma$  can be easily calculated and is  $I \approx 7.34 * 10^{-39} g * cm^2$  (see Appendix). The Hamiltonian of the polypeptide chain in our model with nearest neighbor interactions is

$$H = \sum_i \left\{ \frac{I}{2} \left( \frac{dx_i}{dt} \right)^2 + U_{loc}(x_i) + U(x_i; x_{i+1}) \right\} \quad (2)$$

Here  $U_{loc}(x_i)$  includes interactions defining the local potential of the peptide group (namely hydrogen bonds, the so-called torsional potentials and the van der Waals interaction of covalently non-bonded atoms of the peptide group with the atoms of adjacent side chains) defining its separate motion while  $U(x_i; x_{i+1})$  includes the coupling interactions (namely the van der Waals interaction of covalently non-bonded atoms of adjacent peptide groups  $i$  and  $i+1$  and their electrostatic interaction) intermixing the motions of these groups and leading to the rigidity of the peptide chain. It should be stressed that the latter potential also contributes into the separate motion of the peptide groups. We can define the effective on-site potential for such motion as

$$V_{eff}(x_i) = U_{loc}(x_i) + U(x_i; 0) + U(0; x_i) \quad (3)$$

and the coupling interaction potential as

$$U(x_i; x_{i+1}) = U^{vdw}(x_i; x_{i+1}) + U^{el}(x_i; x_{i+1}) \quad (4)$$

Thus the equation of motion is

$$I \frac{d^2 x_i}{dt^2} = -\frac{dU_{loc}(x_i)}{dx_i} - \frac{dU(x_{i-1}; x_i)}{dx_i} - \frac{dU(x_i; x_{i+1})}{dx_i} \quad (5)$$

In the following two sections we consider in details the functions  $U_{loc}(x_i)$  and  $U(x_i; x_{i+1})$ . At doing it we will freely pass back and forth between the variables according to the rule (1) which can be rewritten as

$$\Delta \varphi_i = x_i/2; \quad \Delta \psi_i = x_{i+1}/2 \quad (6)$$

### 3 Coupling interaction defining the rigidity of a polypeptide chain

Both interactions in (4) intermixing the motions of the adjacent peptide groups and contributing to the coupling interaction are described by the central potentials  $W_{mn}^{vdw}(R_{mn}(\varphi_i; \psi_i))$  and  $W_{mn}^{el}(R_{mn}(\varphi_i; \psi_i))$  between the atom  $A_n$  of the  $i$ -th peptide group and the atom  $A_m$  of the  $i + 1$ -th one with  $R_{mn}$  being the distance between the atoms  $A_n$  and  $A_m$ . The electrostatic potential is

$$W_{mn}^{el}(R_{mn}) = \frac{q_m q_n}{\varepsilon R_{mn}} \quad (7)$$

where  $q_m$  and  $q_n$  are partial charges on the atoms  $A_m$  and  $A_n$  respectively ( $q(N) = -0.28e$ ;  $q(H) = 0.28e$ ;  $q(O) = -0.39e$ ;  $q(C) = 0.39e$  where  $e = 4.8 \times 10^{-10}$  CGS [57]) and  $\varepsilon$  is the dielectric constant which for protein interior should be better conceived as some adjustable parameter ( $\approx 2 \div 10$  with 3.5 being commonly accepted value close to high frequency permeability of peptides) [57], [8]. In some studies  $\varepsilon$  is supposed to be solvent dependent and chosen, e.g., 4 for  $CCl_4$ ,  $6 \div 7$  for  $CHCl_3$  and 10 for  $H_2O$  [58], [59]. For the van der Waals potential one can choose any of the numerous forms suggested in the literature, e.g., the Lennard-Jones one (6-12) or the Buckingham one (6-exp). In this chapter we use for numerical estimates the former one

$$W^{vdw}(R_{mn}) = -\frac{A_{mn}}{R_{mn}^6} + \frac{B_{mn}}{R_{mn}^{12}} \quad (8)$$

with the set of the well known parameters of Scott and Scheraga (other sets were also verified and found to give similar results).

The distance  $R_{mn}$  as a function of the angles  $\varphi_i$  and  $\psi_i$  is

$$R_{mn}(\varphi_i, \psi_i) = \{p_m^2 + r_n^2 + 2p_m r_n [\sin \theta (\cos \gamma_m \sin \alpha_n \cos \varphi_i - \sin \gamma_m \cos \alpha_n \cos \psi_i) - \sin \gamma_m \sin \alpha_n (\cos \psi_i \cos \varphi_i \cos \theta - \sin \psi_i \sin \varphi_i) - \cos \gamma_m \cos \alpha_n \cos \theta]\}^{1/2} \quad (9)$$

The interaction potential for both van der Waals and electrostatic interactions has the form

$$U \left\{ \begin{smallmatrix} vdw \\ el \end{smallmatrix} \right\} (x_i; x_{i+1}) = \sum_{mn} W \left\{ \begin{smallmatrix} vdw \\ el \end{smallmatrix} \right\} (R_{mn}(x_i; x_{i+1})) \quad (10)$$

where the summation in  $n$  is over atoms in the  $i$ -th peptide group and that in  $m$  is over atoms in the  $i + 1$ -th one.

In what follows we work with full realistic coupling interaction potential described above. However for making use of suggestive analogies with the known literature results obtained on toy models we calculate the so called coupling constant which is a key characteristic of the truncated coupling interaction potential. Expanding the potential we obtain that to the leading order in the terms  $x_i \ll 1$  and  $x_{i+1} \ll 1$  the rigidity of the peptide chain is determined by the term of the potential which intermixes the motion of the adjacent peptide groups

$$U^{mix}(x_i; x_{i+1}) \approx (-K)x_i x_{i+1} \quad (11)$$

where the coupling constant is

$$-K = -(K^{vdw} + K^{el}) = \frac{\partial^2 U^{vdw}(x_i; x_{i+1})}{\partial x_i \partial x_{i+1}} \Big|_{x_i=0; x_{i+1}=0} + \frac{\partial^2 U^{el}(x_i; x_{i+1})}{\partial x_i \partial x_{i+1}} \Big|_{x_i=0; x_{i+1}=0} \quad (12)$$

The results of calculations of the contributions into the coupling constant for the antiparallel  $\beta$ -sheet are as follows:  $\varphi_i^0 = -139^\circ$ ;  $\psi_i^0 = 135^\circ$  [57]:  $-K^{vdw} \approx -5.0 \cdot 10^{-16}$  erg;  $-K^{el} \approx 2.64 \cdot 10^{-15}$  erg;  $-K \approx 2.14 \cdot 10^{-15}$  erg at  $\varepsilon = 3.5$ .

## 4 Local on-site potential of the peptide group

The local potential  $U_{loc}(x_i)$  is composed as follows

$$U_{loc}(x_i) = U_{sc}(x_i) + U_{hb}(x_i) + U_{tors}(x_i) \quad (13)$$

Here  $U_{sc}(x_i)$  is the energy of van der Waals interactions of the atoms of the  $i$ -th peptide group with those of the side chains  $R_i$  and  $R_{i-1}$  and also with the atoms  $H_\alpha^i$  and  $H_\alpha^{i-1}$ ,  $U_{hb}(x_i) = U_{hb}^{(1)}(x_i) + U_{hb}^{(2)}(x_i)$  is the energy of two hydrogen bonds of the  $i$ -th peptide group and  $U_{tors}(x_i) = U_{tors}^\varphi(\varphi_i) + U_{tors}^\psi(\psi_{i-1})$  is the energy of the torsional potentials for the rotation of the angles  $\varphi_i$  and  $\psi_{i-1}$ . For the latter we take the usual form

$$\begin{aligned} U_{tors}^\varphi(\varphi_i) &= E_\varphi(1 + \cos 3\varphi_i) \\ U_{tors}^\psi(\psi_i) &= E_\psi(1 + \cos 3\psi_i) \end{aligned} \quad (14)$$

with  $E_\varphi \approx 1$  kcal/mol and  $E_\psi \approx 1$  kcal/mol. In all further simulations we choose the side chain to be Ala ( $R_i$  is  $C_\beta^i(H)_3$ ) and initially find the value of the angle  $\chi_1$  (see Fig.1) to minimize the energy.

## 5 Hydrogen bond potential

In (13)  $U_{hb}^{(j)}(x_i)$  ( $j=1,2$ ) are the contributions of two hydrogen bonds which a peptide group in the anti-parallel  $\beta$ -sheet forms with its partners. We start from a model Morse potential usually employed to describe the hydrogen bond energy dependence on its current length [58], [59]

$$U_{hb}(x_i) = D(1 - \exp[-n(r(x_i) - r_0)])^2 - D \quad (15)$$

Here  $n \approx 3 \text{ \AA}^{-1}$  and  $r_0 \approx 1.8 \text{ \AA}$  are adjustable parameters for distance dependence and  $D$  is an adjustable parameter of the hydrogen bond energy. For WHB  $D \approx 4 \div 6$  kcal/mol at  $\varepsilon = 3.5$  with  $D = 5$  kcal/mol being a conventional value [8] (in [59]  $D$  is assumed to be a decreasing value at increasing  $\varepsilon$  with  $D = 0.5$  kcal/mol at  $\varepsilon = 10$ ). Finally  $r(x_i)$  is the current length of the hydrogen bond.

We denote  $a^{(j)}$  the distance from the axis  $\sigma$  (see Fig.2) to the carbonyl oxygen atom ( $j = 1$  so that  $a^{(1)} \approx 1.5 \text{ \AA}$  (see Appendix)) or that to the hydrogen



atom ( $j = 2$  so that  $a^{(2)} \approx 2 \text{ \AA}$  (see Appendix)). Then the current length is related to the angle  $x_i$  by straightforward trigonometry

$$\left(r^{(j)}(x_i^{(j)})\right)^2 = \left(l^{(j)}\right)^2 + 4\left(a^{(j)}\right)^2 \left(\sin(x_i^{(j)}/4)\right)^2 \left[a^{(j)} + l^{(j)} \cos \theta^{(j)}\right]$$

This expression takes into account that the range for the angular displacement  $x_i$  (defined in (1)) is  $4\pi$  because it is twice of the torsional angles  $\varphi_i$  and  $\psi_{i-1}$  (see (1)). However we also want to take into account that the current length decreases with the increase of the hydrogen bond energy. We attain it by introducing a linear dependence factor  $(1 - qD)$  in the expression for the current length where  $q$  is an empirical parameter

$$r^{(j)}(x_i^{(j)}) = (1 - qD^{(j)}) \times \sqrt{\left(l^{(j)}\right)^2 + 4\left(a^{(j)}\right)^2 \left(\sin(x_i^{(j)}/4)\right)^2 \left[a^{(j)} + l^{(j)} \cos \theta^{(j)}\right]}$$

Thus for the  $U_{hb}^{(j)}(x_i^{(j)})$  ( $j=1,2$ ) we obtain

$$U_{hb}^{(j)}(x_i^{(j)}) = -D^{(j)} + D^{(j)} \left\{ 1 - \exp \left[ -n \left( -r_0^{(j)} + (1 - qD^{(j)}) \times \sqrt{\left(l^{(j)}\right)^2 + 4\left(a^{(j)}\right)^2 \left(\sin(x_i^{(j)}/4)\right)^2 \left[a^{(j)} + l^{(j)} \cos \theta^{(j)}\right]} \right) \right] \right\}^2 \quad (16)$$

Here  $n = 3 \text{ \AA}^{-1}$  and  $r_0 = 1.8 \text{ \AA}$  are old adjustable parameters while  $q$  and  $l^{(j)}$  are two new ones. The latter can be evaluated from the following data obtained in [60]. A  $0.5 \text{ \AA}$  lengthening of the low-barrier hydrogen bond results in a weakening of that bond by over 6 kcal/mol. A  $1.0 \text{ \AA}$  lengthening of the hydrogen bond results in an approximately 12 kcal/mol decrease in the calculated strength of the corresponding hydrogen bond. Taking the energy of the low-barrier hydrogen bond to be  $D = 15 \text{ kcal/mol}$  we obtain from these requirements and (16) that  $q \approx 0.01 \text{ mol/kcal}$  and  $l^{(j)} \approx 2.0 \text{ \AA}$ . The angles  $\theta^{(1)}$  and  $\theta^{(2)}$  can be evaluated from the known data on the bond lengths and angles in the peptide group [57] as  $\theta^{(1)} \approx \theta^{(2)} \approx 30^\circ$ .

## 6 Effective on-site potential and coupling interaction potential

The adjustable parameters are chosen to satisfy the following set of requirements: 1. The effective on-site potential  $V_{eff}(x_i)$  (see 3) must have a minimum at equilibrium ( $x_i = 0$ ) because the antiparallel  $\beta$ -sheet is a steady stable

structure. 2. For the anti-parallel  $\beta$ -sheet the hydrogen bond are known (see, e.g., [9] or [57]) to be practically parallel to the corresponding covalent bonds  $C = O$  and  $N - H$  (see Fig.2). 3. For the anti-parallel  $\beta$ -sheet the spectroscopic frequency

$$(1/\lambda)_{sp} = \frac{\sqrt{V''_{eff}(x_i = 0)/I}}{2\pi c} \quad (17)$$

are  $\sim 100 \text{ cm}^{-1}$ . Here  $\lambda$  is a wavelength,  $c$  is the light speed and the dash denotes a derivative in  $x_i$ .

We take for the anti-parallel  $\beta$ -sheet  $\varphi_i^0 = -139^\circ$ ;  $\psi_i^0 = 135^\circ$  [57]. One hydrogen bond for the peptide group the anti-parallel  $\beta$ -sheet (namely that with  $j = 1$ ) always remains to be WHB ( $D^{(1)} = 5 \text{ kcal/mol}$ ). For the second hydrogen bond we vary the value  $D^{(2)}$  for the energy within the range  $2 \div 30 \text{ kcal/mol}$ .

In what follows we use dimensionless variables. We define the frequency

$$\omega = \sqrt{\frac{V''_{eff}(x_i = 0)}{I}} \quad (18)$$

and measure time in the units of  $\omega^{-1}$  so that the dimensionless time is

$$\tau = t\omega \quad (19)$$

Also we measure energy in the units of  $I\omega^2$  and denote the dimensionless coupling constant  $\rho$

$$\rho = \frac{K}{I\omega^2} \quad (20)$$

## 7 Equation of motion and correlation function for crankshaft motion

In this Sec. we denote for simplicity  $x_i(t) \equiv \phi(t)$  and rewrite (1) in the form

$$\phi/2 \equiv \Delta\varphi_i = \Delta\psi_{i-1} \quad (21)$$

It is natural to describe the crankshaft motion by a Langevin equation. Such equations are frequently used in protein dynamics [61], [62], [63], [64], [65],

[66]. The equation of the crankshaft motion for the rigid plane of the peptide group in the above conditions is

$$I \frac{d^2 \phi(t)}{dt^2} + \gamma \frac{d\phi(t)}{dt} + I\omega_0^2 \phi(t) = \xi(t) \quad (22)$$

where  $\gamma$  is the friction coefficient and  $\xi(t)$  is the random torque with zero mean  $\langle \xi(t) \rangle = 0$  and correlation function

$$\langle \xi(0)\xi(t) \rangle = 2k_B T \gamma \delta(t) \quad (23)$$

$k_B$  is the Boltzman constant,  $T$  is the temperature.

We consider the hydrodynamic friction. This "macroscopic" notion is known to work surprisingly well at the molecular level (see [67] for thorough discussion). We model the peptide group by an oblate ellipsoid with half-axes  $a$ ,  $b$  and  $c$  (where  $a \sim c$  and  $a, c \gg b$  that reflects the flat character of the peptide group) Fig.8. For the rotation of the ellipsoid around  $x$ -axis (that is in our case actually the axis  $\sigma$  for the peptide group introduced above) the friction coefficient is given by a formula [68]

$$(\gamma)_x = 8\pi\eta abc \left[ \frac{12r}{a} + \frac{(bc)^{1/4}}{a^{1/2} \left(1 + \frac{4r}{a^{1/2}(bc)^{1/4}}\right)^3} \right]^{-1} \quad (24)$$

where  $r = 2(abc)^{1/3}$  and  $\eta$  is the viscosity of the ellipsoid environment. The required behavior is obtained if we have the condition of the underdamped motion

$$\frac{\gamma}{I\omega_0} \ll 1 \quad (25)$$

At such requirement we obtain (see e.g. [69], [63])

$$\alpha(t) \equiv \langle \phi(0)\phi(t) \rangle \approx \frac{k_B T}{I\omega_0^2} \exp\left(-\frac{\gamma |t|}{2I}\right) \cos(\omega_0 t) \quad (26)$$

We denote

$$\mu = \frac{\gamma}{\sqrt{2}I\omega_0} \quad (27)$$

Then the Fourier spectrum for the correlation function  $\alpha(t)$  is

$$\tilde{\alpha}(\omega) = \frac{k_B T}{I \omega_0^2} \frac{\mu}{\pi} \frac{1 + \mu^2 + (\omega/\omega_0)^2}{\mu^4 + 2\mu^2 [1 + (\omega/\omega_0)^2] + [1 - (\omega/\omega_0)^2]^2} \quad (28)$$

At our requirement (25) it has a sharp resonance peak at the frequency  $\omega_0$ . For the mean squared amplitude (*msa*) we have

$$msa = \frac{k_B T}{I \omega_0^2} \quad (29)$$

The latter means that the amplitude of the crankshaft motion at room temperature and, e.g., typical value  $\omega_0 \approx 10^{13} s^{-1}$  is

$$\phi_{max} = \sqrt{\frac{k_B T}{I \omega_0^2}} \approx 0.1 \approx 6^\circ \quad (30)$$

that is  $\Delta\varphi_i = \Delta\psi_{i-1} \approx 3^\circ$ . This value sheds light on the origin of essentially vibrational character of the peptide group motion manifested itself in (26) and (28). At such angles of rotational deviation of the peptide group from its mean averaged position the linear displacements of the atoms are  $\sim c \cdot \phi_{max} \approx 0.1 \text{ \AA}$  that is much less than both the size of a solvent molecule and interatomic distances to neighbor fragments of protein structure. That is why the environment exerts rather weak friction for such type of the peptide group motion that is reflected in the requirement (25). Thus we conclude that the thermally equilibrium crankshaft motion of the peptide group is of essentially vibrational character even in such condensed medium as protein interior. Our model yields for the correlation function of the crankshaft motion the exponentially decaying oscillations (26). This type of behavior is in qualitative agreement with the results of molecular dynamics simulations [54].

## 8 Results and discussion

The effective on-site potential for the peptide group in the anti-parallel  $\beta$ -sheet for the case of one weak hydrogen bond ( $D^{(1)} = 5 \text{ kcal/mol}$ ) and one strong hydrogen bond ( $D^{(2)} = 30 \text{ kcal/mol}$ ) is presented in Fig.4. In Fig. 5 the dependence of the spectroscopic frequency of crankshaft motion  $(1/\lambda)_{sp}$  (see (17)) for the peptide group in the antiparallel  $\beta$ -sheet on the energy of one of its hydrogen bonds (namely  $D^{(2)}$ ) at different values of the torsional potentials for the rotation of the angles  $\varphi_i$  and  $\psi_{i-1}$  (see (14)) is depicted. This Fig. shows that at transformation WHB  $\rightarrow$  SHB of WHB with energy 5 kcal/mol into SHB

with energy say  $15 \div 20$  kcal/mol the frequency of crankshaft motion becomes roughly twice of what it was ( $(1/\lambda)_{sp} \approx 40 \text{ cm}^{-1} \rightarrow (1/\lambda)_{sp} \approx 80 \text{ cm}^{-1}$ ). In Fig. 6 the dependence of the dimensionless coupling constant  $\rho$  (see (20)) for the peptide group in the antiparallel  $\beta$ -sheet on the energy of one of its hydrogen bonds (namely  $D^{(2)}$ ) at different values of the torsional potentials for the rotation of the angles  $\varphi_i$  and  $\psi_{i-1}$  (see (14)) is depicted. The dimensionless coupling constant decreases in absolute value with the increase of  $D^{(2)}$  because it is inversely proportional to the  $\omega^2$  (see (20)) while the latter increases with the increase of  $D^{(2)}$  (see Fig. 6). The dimensional value of the coupling constant  $K$  remains unchanged with variation of  $D^{(2)}$  because does not depend on the hydrogen bond potential (see (12)). In Fig.7 the dependence of the coupling constant  $\rho$  (see (20)) for the peptide group in the antiparallel  $\beta$ -sheet on the dielectric constant  $\epsilon$  at different values of the energy of one of its hydrogen bonds (namely  $D^{(2)}$ ) is depicted. This Fig. shows that the dependence of the coupling constant  $\rho$  (see (20)) for the peptide group in the antiparallel  $\beta$ -sheet on the dielectric constant  $\epsilon$  is rather strong. On the other hand the dependence of the frequency of crankshaft motion for the peptide group in the antiparallel  $\beta$ -sheet on the dielectric constant  $\epsilon$  is negligibly small. This can be explained as follows. The frequency of crankshaft motion is determined by the the effective on-site potential (see 3 and 13) that does not include electrostatic interactions while the coupling constant is determined by the coupling interaction potential (see 12 and 20) that strongly depends on electrostatic interactions and thus very sensitive to the value of  $\epsilon$ .

Our results of the investigation of the effective on-site potential and the coupling interaction potential for the anti-parallel  $\beta$ -sheet testify the following: 1. For the anti-parallel  $\beta$ -sheet the coupling interaction is surprisingly weak  $|\rho| \ll 1$  (though the same is true for other types of protein secondary structure [55]). 2. The effective on-site potential is hard (goes more steep than a harmonic one). 3. The coupling interaction is repulsive  $\rho < 0$  at reasonable values of the dielectric constant  $\epsilon < 15$  (the latter means that a non-zero value of a peptide group displacement tends to increase the values of the neighboring peptide groups displacements with the opposite sign). The weakness of the coupling interaction  $|\rho| \ll 1$  is known to be indispensable for the possibility of creation and existence of a specific excitation (the so-called discrete breather) in a chain of non-linear oscillators. Thus we conclude that in the anti-parallel  $\beta$ -sheet a discrete breather can be excited.

The fact that dimensionless values of the coupling constant  $\rho$  are very small, i.e.,  $|\rho| \ll 1$  (see Fig.6 and Fig.7) means that there is little interdependence in the rocking (i.e., Crankshaft motion  $\Delta\varphi_i = \Delta\psi_{i-1}$ ) of the planes of the adjacent peptide groups in the antiparallel  $\beta$ -sheet. This result is in agreement with the conclusion of the authors of [54] that "only a slight correlation is found between the motions of the two backbone dihedral angles of the same residue" (i.e.,  $\Delta\varphi_i$  practically does not correlate with  $\Delta\psi_i$ ).

The most intriguing question is how the transformation of WHB into SHB in the antiparallel  $\beta$ -sheet of the nonspecific binding site of serine proteases can be related to the mechanism of enzyme action? The hypothesis that such relationship can take place was suggested in [3] (see Introduction). In our opinion it is very interesting and requires discussion and further development. The indispensable first step is the storage of the energy released at such transformation. The second step is the transmission of this energy to the scissile bond in the substrate molecule. There are several possible mechanisms of such storage in the antiparallel  $\beta$ -sheet. One of them makes use of the phenomenon of the so-called discrete breather. This possibility was discussed in [55], [70]. The energy of the discrete breather can be transmitted to the scissile bond in the substrate molecule by the electric field fluctuations [70]. Another interesting possibility is the excitation at the WHB  $\rightarrow$  SHB transformation of the self-trapped Amide-I vibration in the  $C = O$  stretching mode of the nearest to the active center peptide group in the antiparallel  $\beta$ -sheet of the nonspecific binding site of serine proteases. Indeed the Amide-I quantum energy is known to be 0.205 eV (see, e.g., [57]), i.e.,  $\approx 4.7$  kcal/mol. Thus the transformation of a WHB  $N - H \cdots O = C$  with energy 5 kcal/mol into a low-barrier hydrogen bond  $N - H \bullet \bullet \bullet O = C$  with energy, e.g, 15 kcal/mol releases enough energy to excite Amide-I of the  $C = O$  bond. Of course one should keep in mind that there can be complications due to the fact that the bond between  $C$  and  $O$  atoms in a peptide group is only partially double one (see, e.g., [57] or [9]). However these complications do not seem to be crucial. If the  $C = O$  vibration is excited then the energy can be transmitted to the scissile bond  $C_{carbonyl} - N$  in the peptide group of the substrate molecule by the nonradiative resonant interaction of the dipole moment  $\bar{d}$  of the stretching mode with that of the  $C_{carbonyl} = O$  bond adjacent to  $C_{carbonyl} - N$ . At the oversimplifying approximation that both dipoles have equal tilt relative the axis  $z$  connecting them the exchange energy (vibrational coupling) of the dipole-dipole interaction  $J$  can be evaluated as [71], [72]

$$J = \frac{\bar{d}^2}{R^3} (3 \cos^2 \theta - 1)$$

Here  $R$  is the distance between the  $C = O$  bonds and  $\theta$  is the angle between the dipole moment  $\bar{d}$  and the axis  $z$ . The value of  $J$  for, e.g., peptide groups in  $\alpha$ -helix was estimated from experimental data of infrared spectra and it was found that  $J = 1.55 \cdot 10^{-22}$  Joule [73], i.e.,  $J \approx 2.22 \cdot 10^{-2}$  kcal/mol. Thus the Hamiltonian for two interacting  $C = O$  bonds can be written as

$$H_{ex} = \hbar\omega_0 \sum_{n=1}^2 a_n^+ a_n - J \sum_{n=1}^2 (a_n^+ a_{n+1} + a_n a_{n+1}^+)$$

where  $\omega_0$  is the frequency of Amide-I ( $\sim 1600$   $cm^{-1}$ ) and  $a_n^+$  ( $a_n$ ) is the creation

(annihilation) operator for an Amide-I exciton in the site  $n$ . The storage of vibrational energy in the  $C = O$  stretching mode is widely used within the framework of the Davydov model for the bio-energy transport in a polypeptide chain [71], [72]. In this model the  $C = O$  vibration is excited by the energy released in the adenosine triphosphate (ATP) hydrolysis that yields about 0.43 eV. Hamiltonian of the above type is still a matter intensive investigations within the context of energy transfer in proteins (see, e.g., [74] and refs. therein). Regretfully we failed to find experimental or theoretical investigations of the key point for our hypothetical scenario namely that of Amide-I excitation at transformation of the ordinary hydrogen bond into low-barrier ones. That is why we restrict ourselves from further discussing this speculation and leave the development of posed above possibility for future work.

The conclusions of the paper are summarized as follows. The dynamics of a peptide chain in the anti-parallel  $\beta$ -sheet is considered within a realistic model with stringent microscopically derived coupling interaction potential and effective on-site potential. The coupling interaction is found to be surprisingly weak and repulsive in character. The effective on-site potential is found to be a hard one. At transformation of ordinary hydrogen bond into low-barrier one the frequency of crankshaft motion of the corresponding peptide group in the anti-parallel  $\beta$ -sheet is roughly doubled.

Acknowledgements. The author is grateful to Prof. Yu.F. Zuev and Dr. B.Z. Idiyatullin for helpful discussions. The work was supported by the grant from RFBR and the programme "Molecular and Cellular Biology" of RAS.

## 9 Appendix A

Here we give a brief estimate of the moment of inertia of the peptide group for rotation around the axis  $\sigma$  that goes through the center of masses of the peptide group parallel to the bonds  $C_{\alpha}^{i-1} - C^i$  and  $N^i - C_{\alpha}^i$  (see Fig.2). The peptide group is a rigid plane structure so that all atoms  $O$ ,  $C$ ,  $N$  and  $H$  lie in a plane. That is why the moment of inertia is simply the sum of their masses multiplied by the square of their distances to the axis  $\sigma$ . The masses in atomic units ( $1 \text{ a.u.m.} = 1.7 \cdot 10^{-24}g$ ) are  $m_O = 16$ ,  $m_C = 12$ ,  $m_N = 14$  and  $m_H = 1$ . That is why the center of masses is shifted a little to the atoms  $C$  and  $O$  relative the middle of the bond  $C - N$ . The lengths of the bonds are  $l_{OC} = 1.24 \text{ \AA}$ ,  $l_{CN} = 1.32 \text{ \AA}$  and  $l_{NH} = 1.0 \text{ \AA}$ . That is why the distances to the axis  $\sigma$  are approximately  $r_O \approx 1.5 \text{ \AA}$ ,  $r_C \approx 0.3 \text{ \AA}$  and  $r_N \approx 0.7 \text{ \AA}$  and  $r_H \approx 2 \text{ \AA}$ . Substituting these values into the formula  $I = \sum m_i r_i^2$  we obtain  $I \approx 7.6 \cdot 10^{-39}g \cdot cm^2$ . Thus our rough estimate corroborate the precise value  $I \approx 7.34 \cdot 10^{-39}g \cdot cm^2$  from [75].

## References

- [1] Zhou H-X, Gilson MK (2009) Theory of free energy and entropy in noncovalent binding. *Chem. Rev.* 109: 4092-4107.
- [2] Schreiber G, Haran G, Zhou HX (2009) Fundamental aspects of protein-protein association kinetics. *Chem. Rev.* 109: 839-860.
- [3] Fodor K, Harmat V, Neutze R, Szilágyi L, Gráf L, Katona G (2006) Enzyme:substrate hydrogen bond shortening during the acylation phase of serine protease catalysis. *Biochemistry* 45: 2114-2121.
- [4] Bone R, Fujishige A, Kettner CA, Agard DA (1991) Structural basis for broad specificity in  $\alpha$ -lytic protease mutants. *Biochemistry* 30, 10388-10398.
- [5] Fuhrmann CN, Daugherty MD, Agard DA (2006) Role of short H-bonds in  $\alpha$ -lytic protease catalysis. *J.Am.Chem.Soc.* 128: 9086-9102.
- [6] Hedstrom L (2002) Serine protease mechanism and specificity. *Chem. Rev.* 102: 4501-4523.
- [7] Polgár L (2005) The catalytic triad of serine peptidases. *Cell. Mol. Life Sci.* 62: 2161-2172.
- [8] Finkelstein AV, Ptitsyn OB (2002) *Physics of protein*. University: Moscow.
- [9] Branden C, Tooze J (1999) *Introduction to protein structure*. 2-nd ed. Garland Publishing, Inc.
- [10] Cleland WW, Frey PA, Gerlt JA (1998) The low barrier hydrogen bond in enzymatic catalysis. *J.Biol.Chem.* 273: 25529-25532.
- [11] Frey PA (2004) Low barrier hydrogen bonds. *Encyclopedia of Biological Chemistry* 2: 594-597.
- [12] Warshel A, Papazyan A (1996) Energy considerations show that low-barrier hydrogen bonds do not offer catalytic advantage over ordinary hydrogen bonds. *Proc.Natl.Acad. Sci. USA* 93: 13665-13670.
- [13] Shokhen M, Albeck A (2004) Is there a weak H-bond  $\rightarrow$  LBHB transition on tetrahedral complex formation in serine proteases? *Proteins: Structure, Function and Bioinformatics* 54: 468-477.
- [14] Cleland WW (1992) Low-barrier hydrogen bonds and low fractionation factor bases in enzymic reactions. *Biochemistry* 31:317-319.
- [15] Cleland WW, Kreevoy MM (1994) Low-barrier hydrogen bonds and enzymic catalysis. *Science* 264:1887-1890.
- [16] Frey PA, Whitt SA, Tobin JB (1994) A low-barrier hydrogen bond in the catalytic triad of serine proteases. *Science* 264:1927-1930.
- [17] Frey PA (1995) Low-barrier hydrogen bonds. *Science* 268:189.



- [18] Gerlt JA, Kreevoy MM, Cleland WW, Frey PA (1997) Understanding enzymic catalysis: the importance of short, strong hydrogen bonds. *Chem.Biol.* 4:259-267.
- [19] Cassidy CS, Lin J, Frey PA (1997) A new concept for the mechanism of action of chymotrypsin: the role of the low-barrier hydrogen bond. *Biochemistry* 36:4576-4584.
- [20] Cleland WW (2000) Low-barrier hydrogen bonds and enzymic catalysis. *Arch.Biochem.Biophys.* 382:1-5.
- [21] Ha N-C, Kim M-S, Lee W, Choi KY, Oh B-H (2000) Detection of large pKa perturbations of an inhibitor and a catalytic group at an enzyme active site, a mechanistic basis for catalytic power of many enzymes. *J.Biol.Chem.* 275:41100-41106.
- [22] Westler WM, Frey PA, Lin J, Wemmer DE, Morimoto H, Williams PG, Markley JL (2002) Evidence for a strong hydrogen bond in the catalytic dyad of transition-state analogue inhibitor complexes of chymotrypsin from proton-triton NMR isotope shifts. *J.Am.Chem.Soc.* 124:4196-4197.
- [23] Tamada T, Kinoshita T, Kuihara K, Adaci M, Ohhara T, Imai K, Kuroki R, Tada T (2009) Combined high-resolution neutron and X-ray analysis of inhibited elastase confirms the active-site oxyanion hole but rules against a low-barrier hydrogen bond. *J.Am.Chem.Soc.* 131: 11033-11040.
- [24] Karingithi RN, Shaw CL, Roberts EW, Molina PA (2008) The probability distribution function as a descriptor of hydrogen bond strength. *Journal of Molecular Structure: THEOCHEM* 851: 92-99.
- [25] Woutersen S, Hamm P (2002) Nonlinear two-dimensional vibrational spectroscopy of peptides. *J.Phys.- Condensed Matter* 14: R1035-R1062.
- [26] Woutersen S, Hamm P (2001) Time-resolved two-dimensional vibrational spectroscopy of a short alpha-helix in water. *J.Chem.Phys.* 115: 7737-7743.
- [27] Hamm P, Lim MH, Hochstrasser RM (1998) Structure of the amide I band of peptides measured by femtosecond nonlinear-infrared spectroscopy. *J.Phys.Chem.B* 102: 6123-6138.
- [28] Hamm P, Lim MH, DeGrado WF, Hochstrasser RM (2000) Pump/probe self heterodyned 2D spectroscopy of vibrational transitions of a small globular peptide. *J.Chem.Phys.* 112: 1907-1916.
- [29] Xie A, Van der Meer A, Hoff W, Austin RH (2000) Long-lived amide I vibrational modes in myoglobin. *Phys.Rev.Lett.* 84: 5435-5438.
- [30] Xie A, Van der Meer A, Austin RH (2002) Excited-state lifetimes of far-infrared collective modes in proteins. *Phys.Rev.Lett.* 88: 018102.
- [31] Yu X, Leitner DM (2003) Vibrational energy transfer and heat conduction in a protein. *J.Phys.Chem.B* 107: 1698-1707.

- [32] Leitner DM (2002) Anharmonic decay of vibrational states in helical peptides, coils, and one-dimensional glasses. *J.Phys.Chem.A* 106: 10870-10876.
- [33] Leitner DM (2001) Vibrational energy transfer in helices. *Phys.Rev. Lett.* 8718: 8102-8103.
- [34] Karplus M, McCammon JA (2002) Molecular dynamics simulations of biomolecules. *Nature Structural Biol.* 9: 646-652.
- [35] Karplus M (2003) Molecular dynamics of biological macromolecules: A brief history and perspective. *Biopolymers* 68: 350-358.
- [36] Peyrard M ed. (1995) *Nonlinear excitations in biomolecules*. Springer: Berlin.
- [37] Zorski H, Infeld E (1997) Continuum dynamics of a peptide chain. *Int. J.Non-Linear Mechanics* 32: 769-801.
- [38] Zorski H (1999) Model of local rigidity in the theory of peptide chain. *Meccanica* 34: 453-466.
- [39] Merisov JP, Shulter K, De Witt Sumners eds. (1996) *Mathematical approaches to biomolecular structure and dynamics*. Springer: Berlin.
- [40] Go M, Go N (1976) Fluctuations of an  $\alpha$ -helix. *Biopolymers* 15: 1119-1127.
- [41] McCammon JA, Gelin BR, Karplus M (1977) Dynamics of folded proteins, *Nature* 267: 585-590.
- [42] Levy RM, Karplus M (1979) Vibrational approach to the dynamics of an  $\alpha$ -helix. *Biopolymers* 18: 2465-2495.
- [43] Van Gunsteren MF, Karplus M (1982) Protein dynamics in solution and in a crystalline environment: A molecular dynamics study. *Biochemistry* 21: 2259-2274.
- [44] Levitt M (1983) Molecular dynamics of native protein. II. Analysis and nature of motion. *J.Mol.Biol.* 168: 621-657.
- [45] Dellwo MJ, Wand AJ (1989) Model dependent and model independent analysis of the global and internal dynamics of cyclosporin A. *J.Am.Chem.Soc.* 111: 4571-4578.
- [46] Chandrasekhar I, Clore GM, Szabo A, Gronenborn AM, Brooks BR (1992) A 500 ps molecular dynamics simulation study of interleukin-1 in water: correlation with nuclear magnetic resonance spectroscopy and crystallography. *J.Mol.Biol.* 226:
- [47] Palmer AG III, Case DA (1992) Molecular dynamics analysis of NMR relaxation in a zinc-finger peptide. *J. Am. Chem. Soc.* 114: 9059-9067.
- [48] Brunne RM, Berndt KD, Güentert P, Wuëthrich K, Van Gunsteren WF (1995) Structure and internal dynamics of the bovine pancreatic trypsin inhibitor in aqueous solution from longtime molecular dynamics simulations. *Proteins* 23: 49-62.

- [49] Fadel AR, Jin DQ, Montelione GT, Levy RM (1995) Crankshaft motions of the polypeptide backbone in molecular dynamics simulations of human type- $\alpha$  transforming growth factor. *J. Biomol. NMR* 6: 221-226.
- [50] Buck M, Karplus M (1999) Internal and overall peptide group motion in proteins: Molecular dynamics simulations for lysozyme compared with results from X-ray and NMR spectroscopy. *J.Am.Chem.Soc.* 121: 9645-9658.
- [51] Déméné H, Sugàr IP (1999) Protein conformation and dynamics. Effects of crankshaft motions on  $^1\text{H}$  NMR cross-relaxation effects. *J.Phys.Chem. A* 103: 4664-4672.
- [52] Ulmer TS, Ramirez BE, Delaglio F, Bax A (2003) Evaluation of backbone proton positions and dynamics in a small protein by liquid crystal NMR spectroscopy. *J.Am.Chem.Soc.* 125: 9179-9191.
- [53] Clore GM, Schwieters CD (2004) Amplitudes of protein backbone dynamics and correlated motions in a small R/ protein: correspondence of dipolar coupling and heteronuclear relaxation measurements. *Biochemistry* 43: 10678-10691.
- [54] Fitzgerald JE, Jha AK, Sosnick TR, Freed KF (2007) Polypeptide motions are dominated by peptide group oscillations resulting from dihedral angle correlations between nearest neighbors. *Biochemistry* 46: 669-682.
- [55] Sitnitsky AE (2007) Discrete breathers in protein secondary structure, in: *Soft Condensed Matter. New Research.* Ed. Dillon KI, Ch.5: 157-172, Nova.
- [56] Sitnitsky AE (2008) Solvent viscosity dependence for enzymatic reactions. *Physica A* 387: 5483-5497.
- [57] Cantor CR, Schimmel PR (1980) *Biophysical Chemistry.* Freeman: San Francisco, part 1.
- [58] Dashevskii VG (1987) *Conformational analysis of macromolecules.* Nauka: Moscow.
- [59] Popov EM (1997) *Problem of protein.* Nauka: Moscow, v.3.
- [60] Smallwood CJ, McAllister MA (1997) Characterization of low-barrier hydrogen bonds. 7. Relationship between strength and geometry of short-strong hydrogen bonds. The Formic acid-formate anion model system. An ab initio and DFT investigation. *J.Am.Chem.Soc.* 119: 11277-11281.
- [61] Rosskyt PJ, Karplus M (1979) Solvation. A molecular dynamics study of a dipeptide in water. *J.Am.Chem.Soc.* 101: 1913-1937.
- [62] Doster W (2006) Brownian oscillator analysis of molecular motions in biomolecules, in: *Neutron Scattering in Biology, Methods and Applications,* Eds.: Fitter J, Gutberlet T, Katsaras J, Springer, Berlin.
- [63] Rubin AB (2004) *Biophysics,* v.1, Nauka, Moscow, Ch.14.
- [64] Sitnitsky AE (1996) Spectral properties of conformational motion in proteins. *J.Biol.Phys.* 22: 187-196.

- [65] Sitnitsky AE (2000) Modeling the correlation functions of conformational motion in proteins. *J.Biomol.Struct.@Dyn.* 17: 735-745.
- [66] Sitnitsky AE (2002) Modeling the "glass" transition in proteins. *J.Biomol.Struct.@Dyn.* 17: 595-605.
- [67] Metiu H, Oxtoby DW, Freed KF (1977) Hydrodynamic theory for vibrational relaxation in liquids. *Phys.Rev.A* 15: 361-371.
- [68] Klüner RP, Dölle A (1997) Friction coefficient and correlation times for anisotropic rotational diffusion of molecules in liquids obtained from hydrodynamic models and  $^{13}\text{C}$  relaxation data. *J.Phys.Chem. A* 101: 1657-1661.
- [69] Heer CV (1972) Statistical mechanics, kinetic theory and stochastic processes, Academic Press, N.Y., Ch. X.
- [70] Sitnitsky AE (2006) Dynamical contribution into enzyme catalytic efficiency. *Physica A* 371: 481491.
- [71] Davydov AS (1979) Biology and quantum mechanics. Naukova Dumka.Kiev.
- [72] Davydov AS (1984) Solitons in molecular systems. Naukova Dumka.Kiev.
- [73] Nevskay NA, Chirgadze NYu (1976) Infrared spectra and resonance interactions of Amide-I and II vibrations of  $\alpha$ -helix. *Biopolymers* 15: 637-648.
- [74] Kobus M, Nguyen PH, Stock G (2011) Coherent vibrational energy transfer along a peptide helix. *J.Chem.Phys.* 134: 124518.
- [75] Flytzanis N, Savin AV, Zolotaryuk Y (1994) Soliton dynamics in a thermalized molecular chain with transversal degree of freedom. *Phys.Lett.A* 193:148-153.

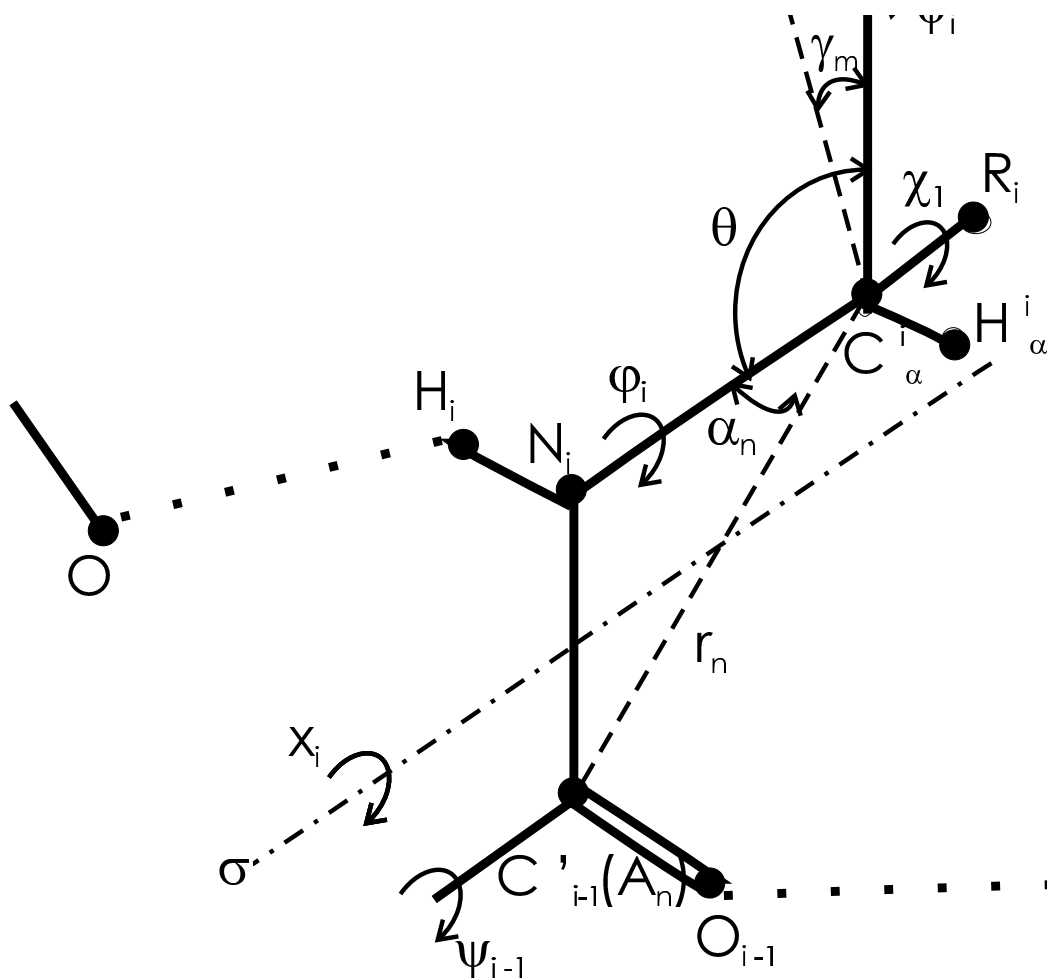


Fig. 1. A schematic representation of the peptide chain with all designations necessary for the text. The covalent bonds are shown as bold lines. Dotted lines denote hydrogen bonds. Dashed lines denote auxiliary axes.

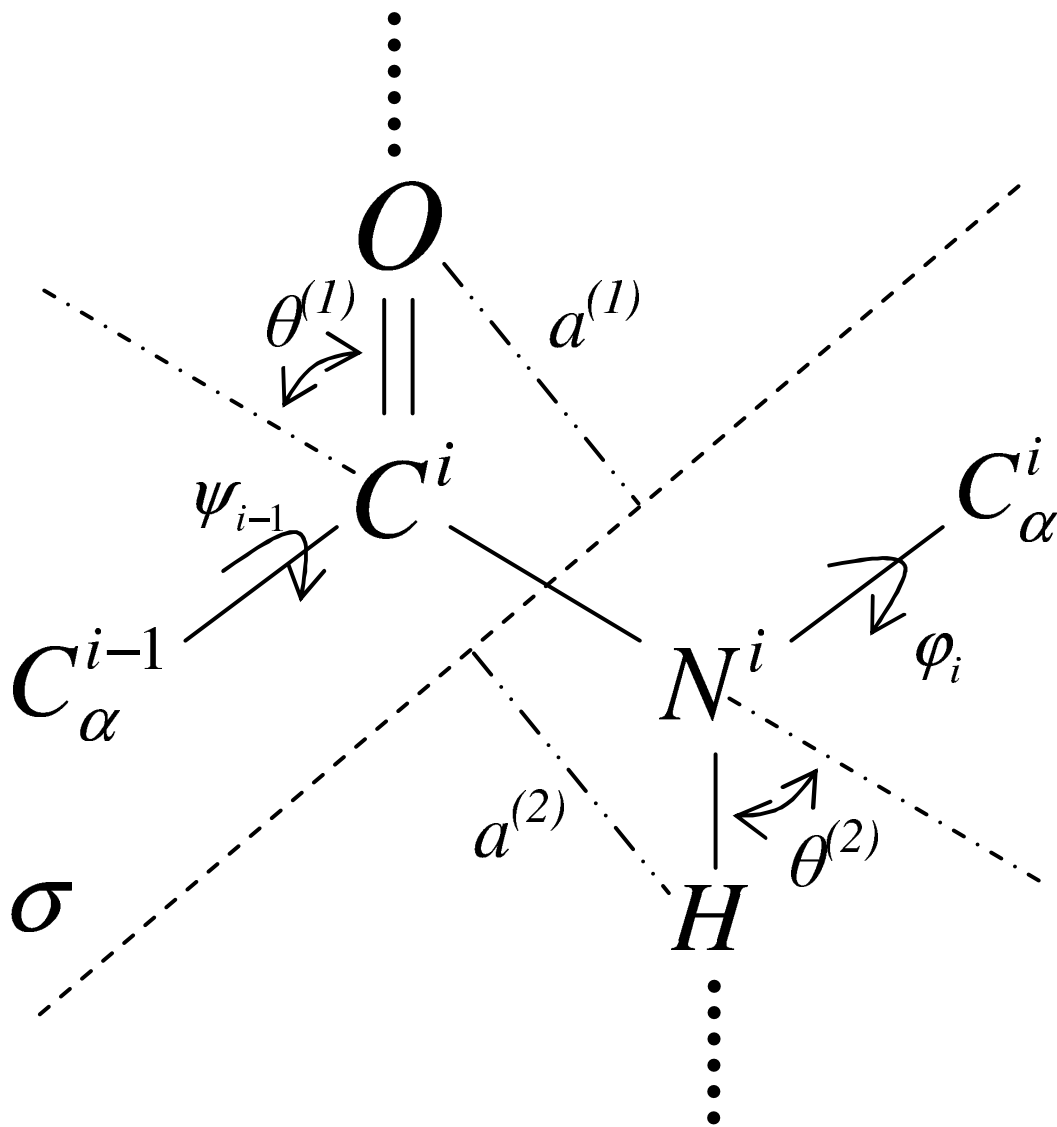


Fig. 2. Schematic picture of the peptide group in the antiparallel  $\beta$ -sheet .

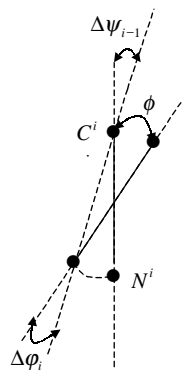


Fig. 3. A look on the peptide group from the axis of rotation  $\sigma$  explaining the definition of the angle  $\phi$  (defined in (3)).

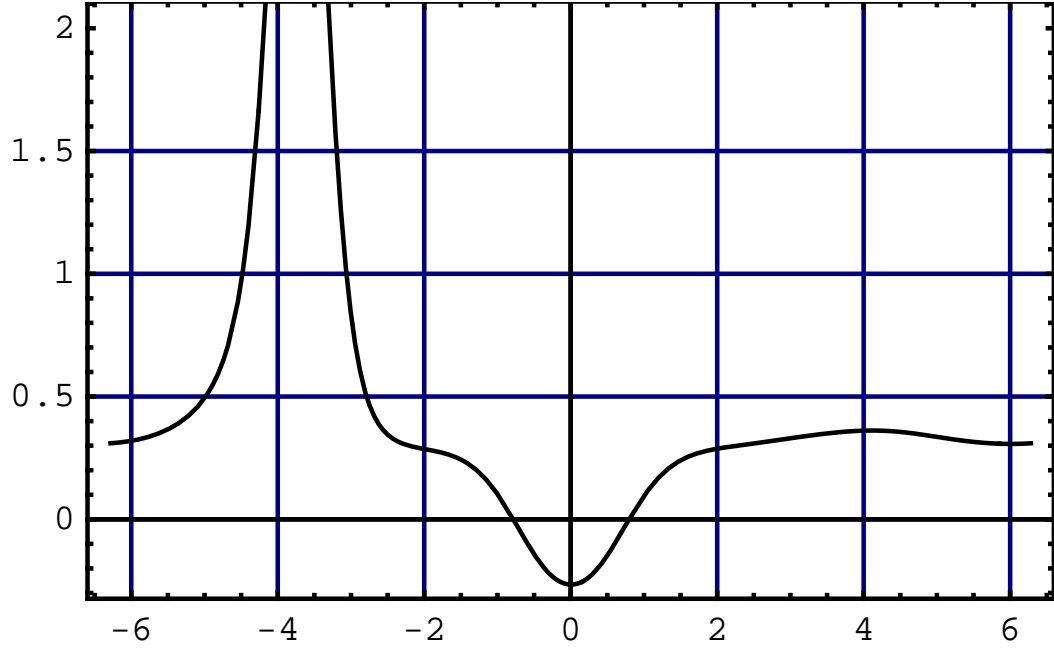


Fig. 4. The normalized effective on-site potential  $V_{eff}(x)$  (see (3)) for the peptide group in the antiparallel  $\beta$ -sheet in case of one weak hydrogen bond ( $D^{(1)} = 5$  kcal/mol) and one strong hydrogen bond ( $D^{(2)} = 30$  kcal/mol). The value of the dielectric constant is  $\varepsilon = 3.5$ . Here  $I$  is the moment of inertia of the peptide group relative the axis  $\sigma$  and  $\omega$  is the frequency. The range for the angular displacement  $x$  (defined in (1)) is  $4\pi$  because it is twice of the torsional angles  $\varphi$  and  $\psi$  (see (1)).



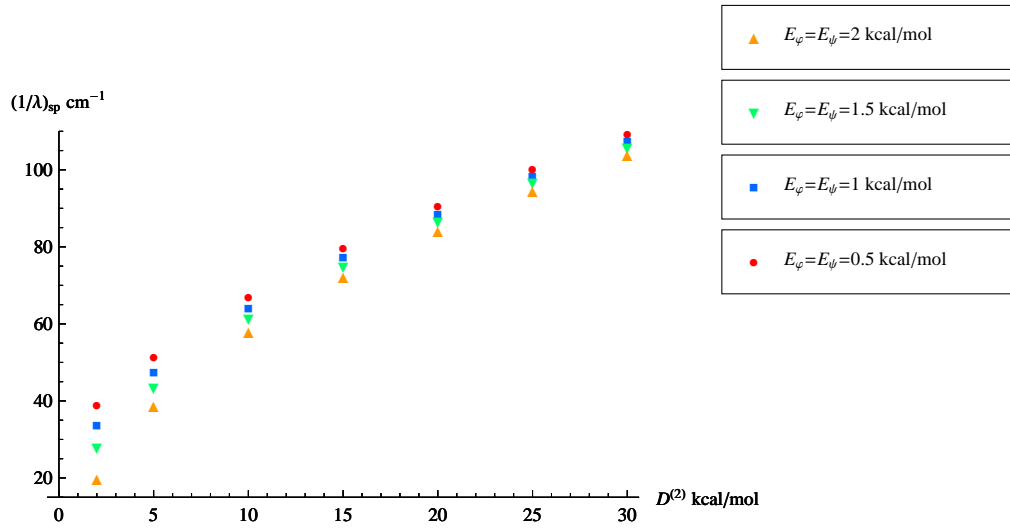


Fig. 5. The dependence of the spectroscopic frequency of crankshaft motion  $(1/\lambda)_{sp}$  (see (17)) for the peptide group in the antiparallel  $\beta$ -sheet on the energy of one of its hydrogen bonds (namely  $D^{(2)}$ ) at different values of the torsional potentials for the rotation of the angles  $\varphi_i$  and  $\psi_{i-1}$  (see (14)):  $E_\varphi = 0.5$  kcal/mol,  $E_\psi = 0.5$  kcal/mol;  $E_\varphi = 1.$  kcal/mol,  $E_\psi = 1.$  kcal/mol;  $E_\varphi = 1.5$  kcal/mol,  $E_\psi = 1.5$  kcal/mol;  $E_\varphi = 2.$  kcal/mol,  $E_\psi = 2.$  kcal/mol. The value of the dielectric constant is  $\varepsilon = 3.5$ .

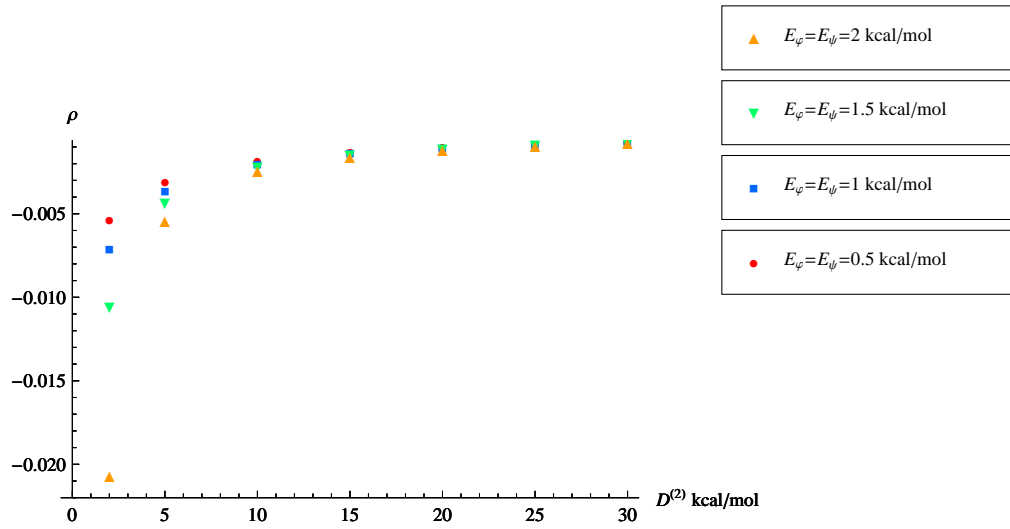


Fig. 6. The dependence of the coupling constant  $\rho$  (see (20)) for the peptide group in the antiparallel  $\beta$ -sheet on the energy of one of its hydrogen bonds (namely  $D^{(2)}$ ) at different values of the torsional potentials for the rotation of the angles  $\varphi_i$  and  $\psi_{i-1}$  (see (14)):  $E_\varphi = 0.5$  kcal/mol,  $E_\psi = 0.5$  kcal/mol;  $E_\varphi = 1$  kcal/mol,  $E_\psi = 1$  kcal/mol;  $E_\varphi = 1.5$  kcal/mol,  $E_\psi = 1.5$  kcal/mol;  $E_\varphi = 2$  kcal/mol,  $E_\psi = 2$  kcal/mol. The value of the dielectric constant is  $\varepsilon = 3.5$ .

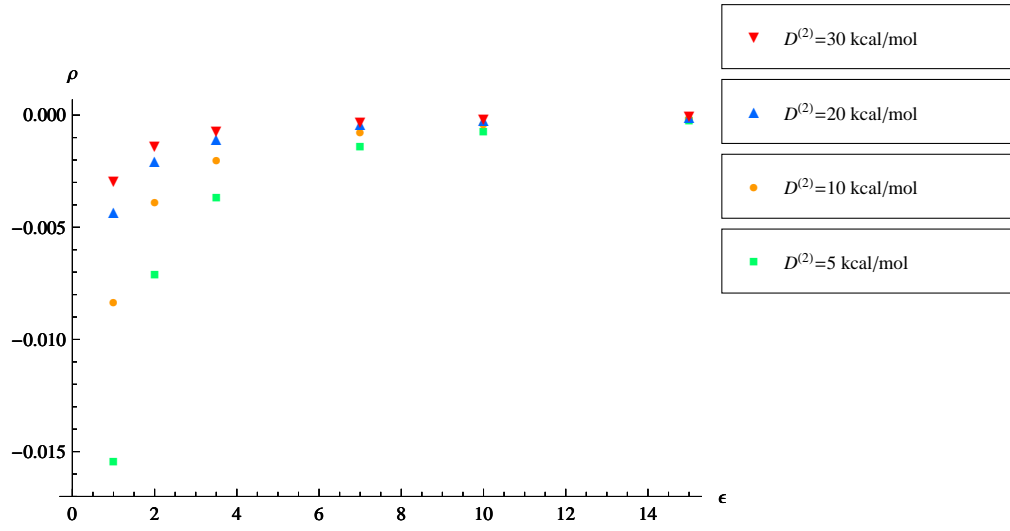


Fig. 7. The dependence of the coupling constant  $\rho$  (see (20)) for the peptide group in the antiparallel  $\beta$ -sheet on the dielectric constant  $\epsilon$  at different values of the energy of one of its hydrogen bonds (namely  $D^{(2)}$ ):  $D^{(2)} = 5$  kcal/mol;  $D^{(2)} = 10$  kcal/mol;  $D^{(2)} = 20$  kcal/mol;  $D^{(2)} = 30$  kcal/mol. The values of the torsional potentials for the rotation of the angles  $\varphi_i$  and  $\psi_{i-1}$  (see (14)) are  $E_\varphi = 1$ . kcal/mol,  $E_\psi = 1$ . kcal/mol.

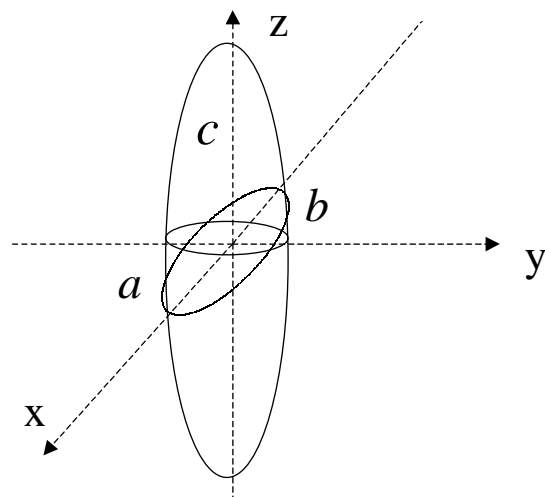


Fig. 8. Model of the peptide group by oblate ellipsoid.